Journal of King Saud University – Engineering Sciences (2018) 30, 339–344

King Saud University

Journal of King Saud University – Engineering Sciences

www.ksu.edu.sa
www.sciencedirect.com

ORIGINAL ARTICLE

The electrical transition temperature and magnetoresistance prediction of $LaSr_2Mn_2O_7$ bilayered manganite

Mohammad Hossein Ehsani *, **Mahmoud Jalali Mehrabad**

Department of Physics, Semnan University, Semnan 35195-363, Iran

Received 20 June 2015; accepted 24 March 2016
Available online 2 April 2016

KEYWORDS

Bilayered manganite;
Magneto-resistance;
Resistivity;
Fitting

Abstract In this paper, the resistivity of bilayer manganite $LaSr_2Mn_2O_7$ around the metal–insulator-like transition was systematically calculated as a function of temperature and applied magnetic field. A typical mathematical function (Gauss function) was used for fitting the experimental data. The theoretical values simulated in this work such as – metal–insulator transition temperature (T_p) and maximum resistivity (ρ_{max}) showed promising agreement with the experimental data.
© 2016 King Saud University. Production and hosting by Elsevier B.V. This is an open access article under the CC BY-NC-ND license (http://creativecommons.org/licenses/by-nc-nd/4.0/).

1. Introduction

The revelation that manganite perovskites demonstrate extreme changes in electrical resistivity upon the application of an external magnetic field is called the colossal magnetoresistance effect (CMR) or the magneto-resistance effect (MR). This can create some technological applications such as magnetic sensors and recording media as well as magnetic refrigerator applications near room temperature in moderated magnetic fields (Ramirez, 1997; Panwar et al., 2015; Isaac et al., 1998; Ehsani et al., 2016, 2013; Liu et al., 2013). The correlation between magnetic and electrical properties was explained via a double exchange (DE) mechanism as a ferromagnetic coupling between the Mn^{3+} ($t_{2g}^3e_g^1$) and Mn^{4+} ($t_{2g}^3e_g^0$) spins which is generally used to explain the CMR phenomena observed in these manganites (Zener, 1951; Goodenough et al., 1955; Anderson and Hasegawa, 1955). Different transport mechanisms have been suggested to explain the semi-conductor-like behavior of resistivity of layered manganites at high temperatures (Nair and Banerjee, 2004; Chen et al., 2002, 2003; Moritomo et al., 1996; Gupta et al., 2007). Studying the temperature dependence of resistivity on doped $La_{2-2x}Sr_{1+2x}Mn_2O_7$ and other layered manganites has been the subject of numerous works (Nair and Banerjee, 2004; Feng et al., 2005; Zhang et al., 2004a,b; Seshadri et al., 1997; Mitchell et al., 2001; Ehsani et al., 2013). The hopping conduction mechanism and its related electrical parameters in the double-layered $LaSr_2Mn_2O_7$ manganite in the intermediate temperature regions $T < \theta_D/2$ and $T > \theta_D/2$ (θ_D is Debye's temperature) have been frequently reported (Feng et al., 2005; Yaremchenko et al., 2008; Ang et al., 2006; Ehsani et al., 2012a,b). However, a model that can describe the carrier transport behavior of manganites as a function of temperature around the electrical phase transition has not been reported.

* Corresponding author. Tel./fax: +98 9123314981.
E-mail address: ehsani@semnan.ac.ir (M.H. Ehsani).
Peer review under responsibility of King Saud University.

Production and hosting by Elsevier

http://dx.doi.org/10.1016/j.jksues.2016.03.004
1018-3639 © 2016 King Saud University. Production and hosting by Elsevier B.V.
This is an open access article under the CC BY-NC-ND license (http://creativecommons.org/licenses/by-nc-nd/4.0/).

Due to several application purposes, evaluation of the parameters such as electrical resistivity (ρ), maximum resistivity (ρ_{max}), and metal–insulator transition temperature (T_p) is considered of great importance (Ramirez, 1997; Panwar et al., 2015; Isaac et al., 1998; Ehsani et al., 2016; Liu et al., 2013; Al-Habahbeh et al., 2018). For example, noticeable changes in magnetic entropy happen around metal–insulator transition temperature (T_p) in magnetic refrigeration (Ehsani et al., 2013). In addition, the correlation between the change of resistivity and T_p shifting due to applied-magnetic field will provide beneficial information for purposes such as designing and examining theoretical models for describing similar materials.

In this paper, the mathematical function proposed by Changshi was used for $La_{0.5}Ca_{0.5}MnO_3$ and $La_{0.8}Sr_{0.2}MnO_3$ manganites (Changshi, 2011). Then, prediction of the metal–insulator transition temperature and maximum electrical resistivity reduction caused by the applied magnetic fields from 0 to 9 T was made.

2. Experimental procedure

$LaSr_2Mn_2O_7$ fine powders were prepared by Pechini sol–gel process. The experimental details for their preparation and characterizations have been reported earlier (Ehsani et al., 2013, 2012a,b). It was found that the samples synthesized at pH = 7 in the sol–gel preparation with the calcination temperature of 1000 °C and sintering temperature 1450 °C had the best growth conditions.

The structural analysis shown in Fig. 1 demonstrated that every X-ray reflection can be indexed using the $Sr_3Ti_2O_7$-type (327-type) tetragonal structure with an I4/mmm space group. Moreover, the morphology of the sample obtained by SEM analysis which can be seen in inset of Fig. 1 confirmed the formation of the continuous grains with micron scale (Ehsani et al., 2012a,b).

As it can be seen from Fig. 2, the energy dispersive analysis of X-ray (EDAX) analysis was performed in order to verify the existence of all elements in the present compound. From the EDAX spectra, La, Sr, Mn, and O can be identified as the constituent elements of all samples, which confirms that there was no loss of any integrated element after the heat treatment.

For the sample, the average La:Sr:Mn:O atomic ratios were found to be 0.083:0.183:0.178:0.55, respectively. The elemental La:Sr:Mn:O ratio is close to the expected ratio (0.08:0.17:0.17:0.58).

For measuring the temperature dependence of resistivity under various applied magnetic fields, the sample with a rectangular shape (2 × 2 × 10 mm) has been put on a standard PPMS (Physical properties measurement system-model 600) sample pucks and, then, the temperature and magnetic field dependence of resistance measurements with high accuracy (±0.0001) were performed. Resistance data were converted systematically to resistivity and the temperature dependence of resistivity was investigated.

3. Results and discussion

Temperature dependent resistivity of $LaSr_2Mn_2O_7$ polycrystalline sample was measured in the applied magnetic field range of $0\ T < B < 9\ T$. The experimental data near the metal–insulator transition temperature within the temperature range of 110 K < T < 210 K are illustrated in Fig. 3.

At temperatures higher than the metal–insulator transition temperature, the resistivity of the specimen was reduced by increasing the temperature, and below the metal–insulator transition temperature was increased by increasing the temperature. The insulating and metallic behaviors of the $LaSr_2Mn_2O_7$ can be clearly observed in Fig. 3 around the transition area.

The metal–insulator transition temperature shifted toward the higher temperatures in the presence of an applied magnetic field and the resistivity magnitude of the specimen was also dramatically reduced.

These behaviors were probably observed, because the spin of the surrounding ions became parallel and disciplined after

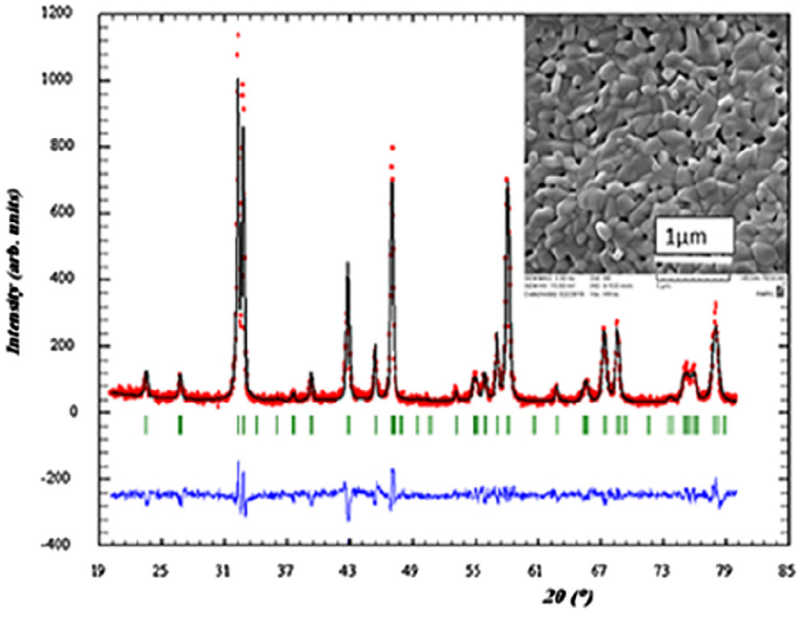

Figure 1 Room temperature XRD patterns (red) and Rietveld profiles (black), inset SEM micrograph of the sample.

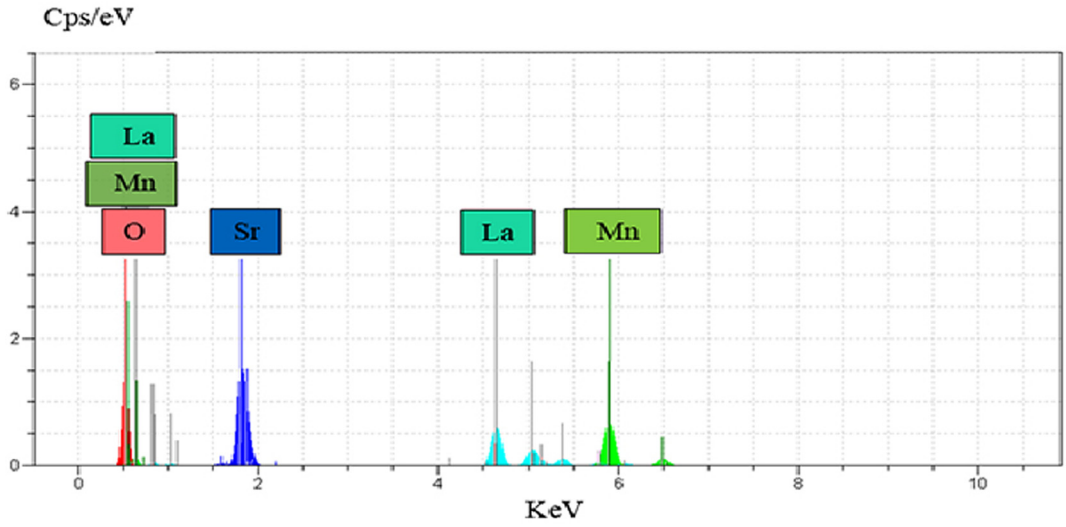

Figure 2 EDAX spectra for sample.

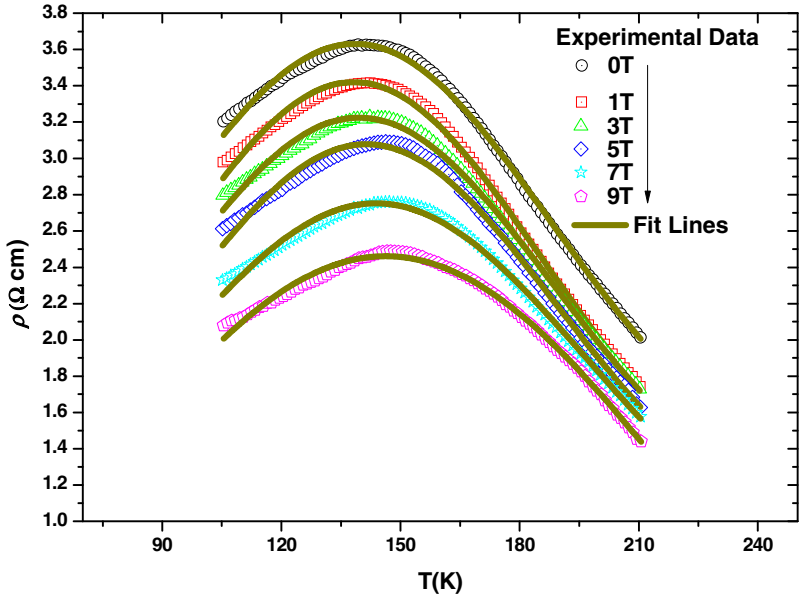

Figure 3 Temperature-field dependent resistivity of $LaSr_2Mn_2O_7$.

applying the magnetic field so that the probability of the electrons hopping from Mn^{3+} to near Mn^{4+} had increased; therefore, the electrical resistivity of the specimen was reduced.

The physical models mentioned in the introduction section are not able to describe the electrical behavior of the specimen near the metal–insulator transition temperature. Therefore, it seems that in order to describe such behaviors for further potential applications, a mathematical model may be used systematically.

Prediction of the magneto resistance of $La_{0.5}Ca_{0.5}MnO_3$ and $La_{0.8}Sr_{0.2}MnO_3$ manganites via temperatures and a magnetic field based on a mathematical approach was reported by Changshi (2011). They used a typical numerical method with a nonlinear curve fitting for the quantitative analysis. According to their suggestion, this approach may be useful for finding or understanding the properties of other manganites using the mathematical method. In this procedure, the Gauss function is used to find a mathematical approach for describing some electrical properties of the specimen.

Gauss function is given in Eq. (1) (Changshi, 2011):

$$\rho(T) = \rho(T_u) + \frac{A}{w\sqrt{\pi/2}} \exp(-2(T/K - T_d/K)^2/w^2) \quad (1)$$

where $\rho(T_u)$ A, T_d, and w are constants obtained from the fitting process.

If the Gauss function is available in order to predict the electrical resistivity (ρ) of $LaSr_2Mn_2O_7$ in all the temperature ranges, then the minimum value of ρ will be given by $\rho(T|_{T\to\infty})$. Therefore, the physical significance of $\rho(T_u)$ is the electrical resistivity of the manganite at high temperatures.

The maximum value for ρ using non-linear fitting is given in Eq. (2):

$$\rho_{\max} = \rho|_{T\to\infty} + \frac{A}{w\sqrt{\pi/2}} \tag{2}$$

Hence, Eq. (1) will be modified as:

$$\rho(T) = \rho_{\min} + \frac{A}{w\sqrt{\pi/2}} \exp(-2(T/K - T_d/K)^2/w^2) \tag{3}$$

The experimental data in Fig. 3 were fitted using Eq. (3). Fitting lines are shown in Fig. 3 and the results are presented in Table 1.

The correlation coefficients (R^2) of the simulated data with experimental data and average relative errors are shown in Table 1. The correlation coefficient, which was close to 1, with a low relative error showed promising correlation between experimental data and the used fitting function. Comparison between the peaks of the experimental data and the magnitude of T_d, calculated from fitting with Gauss function, demonstrated that the behavior of T_d was in good agreement with the metal–insulator transition temperature, T_p.

Therefore, by calculating the appropriate Gauss function form for other magnetic fields, the metal–insulator transition temperature could be simply predicted.

As can be seen from Fig. 3, by increasing the applied magnetic field, the electrical resistivity of the specimen was reduced. Maximum reduction in the magnitude of resistivity occurred around the transition temperature.

Dependency of $\rho_{\max}$ on the applied magnetic field is shown in Fig. 4. The best fitted results demonstrated that the logistic function (4) could properly describe the quantitative relationship between the magnetic field (B) and $\rho_{\max}$ using the nonlinear fitting method.

$$\rho_{\max}(B) = A_1 + \frac{A - A_2}{1 + \left(\frac{B/T}{B_a/T}\right)^p} \tag{4}$$

where A_1, A_2, and B_a are constants and will be calculated using fitting processes. The correlation coefficient between the measured $\rho_{\max}$ which was calculated by fitting was 0.998.

Logistic function (4) properly describes the experimental behavior of maximum electrical resistivity of $LaSr_2Mn_2O_7$. Using this model, it can be seen that maximum electrical resistivity was reduced with increasing the applied magnetic field, which could verify that by increasing the applied magnetic field, the density of the charge carriers would increase; hence, the electrical resistivity of the specimen would be reduced. Therefore, using Eq. (4) for predicting the maximum electrical resistivity, before applying magnetic field, could be very useful to adjust the magnitude of the field. Another application of this approach can be in designing magnetic sensors.

Effect of the magnetic field on metal–insulator transition temperature, T_p, is represented in Fig. 3. As can be seen, by increasing the applied magnetic field, T_p was shifted toward higher temperatures. In the preceding works, it has been seen that T_p of a manganite is related to the applied magnetic field. In order to derive the relationship between T_p and applied magnetic field, the measured values of T_p from Fig. 3 are shown in Fig. 5 as a function of the applied magnetic field, B.

The equation that describes this relationship in two different magnetic field ranges is given by Eq. (5):

$$T_p(B) = \begin{cases} 137.33 + 1.3^{B/T}\ [0, 3T] \\ 139.78 + 0.7816B/T\ [5, 9T] \end{cases} \tag{5}$$

Although the behavior of the magnetic field-dependent T_p shown in Fig. 5 seems to be mathematically complicated, in investigating the spectra of the electrical resistivity of this specimen, it can be seen that data between the magnetic field range of 0–3 T can be fitted very well with the asymptotical Eq. (6):

$$T_p(B) = 137.33 + 1.3^{B/T}\ [0, 3T] \tag{6}$$

The correlation coefficient between the fitted and measured T_p in this range was 0.992.

In higher magnetic fields, the behavior of T_p could be described with linear Eq. (7):

$$T_p(B) = 139.78 + 0.7816B/T[5, 9T] \tag{7}$$

The correlation coefficient between the measured and fitted T_p under the fields higher than 3 to 9 T was 0.956.

Asymptotical equation provides a satisfying description for the relationship between T_p and magnetic field. The shifts of the transition temperature of the specimen caused by the applied magnetic field may occur because of the reduction in the charge barrier delocalization caused by applied magnetic field in weaker fields, which could result in reducing the electrical resistivity of the specimen. The applied magnetic field caused a local spin ordering and because of this ordering, the ferromagnetic state of the metal region could overcome the insulator regiment (charge ordering in this specimen). Therefore, the conducting electrons (e_g^1) were completely polarized within the magnetic domains and could easily trans-

Table 1 Fitting results of experimental data with gauss function.

Applied magnetic field	Calculated gauss function form	R^2	Average relative error %
0	$\rho(T) = 1.16 + \frac{303.9}{98.1\sqrt{\pi/2}}\exp(-2(T/K - 138.5/K)^2/98.1^2)$	0.997	0.25
1	$\rho(T) = 0.97 + \frac{288.2}{94\sqrt{\pi/2}}\exp(-2(T/K - 138.4/K)^2/94^2)$	0.997	0.26
3	$\rho(T) = 0.93 + \frac{274.4}{96.1\sqrt{\pi/2}}\exp(-2(T/K - 139.8/K)^2/96.1^2)$	0.997	0.25
5	$\rho(T) = 0.84 + \frac{265.9}{95.1\sqrt{\pi/2}}\exp(-2(T/K - 141.6/K)^2/95.1^2)$	0.995	0.31
7	$\rho(T) = 0.54 + \frac{296}{107\sqrt{\pi/2}}\exp(-2(T/K - 144.1/K)^2/107^2)$	0.995	0.24
9	$\rho(T) = -1 + \frac{670.6}{154\sqrt{\pi/2}}\exp(-2(T/K - 146.3/K)^2/154^2)$	0.994	0.21

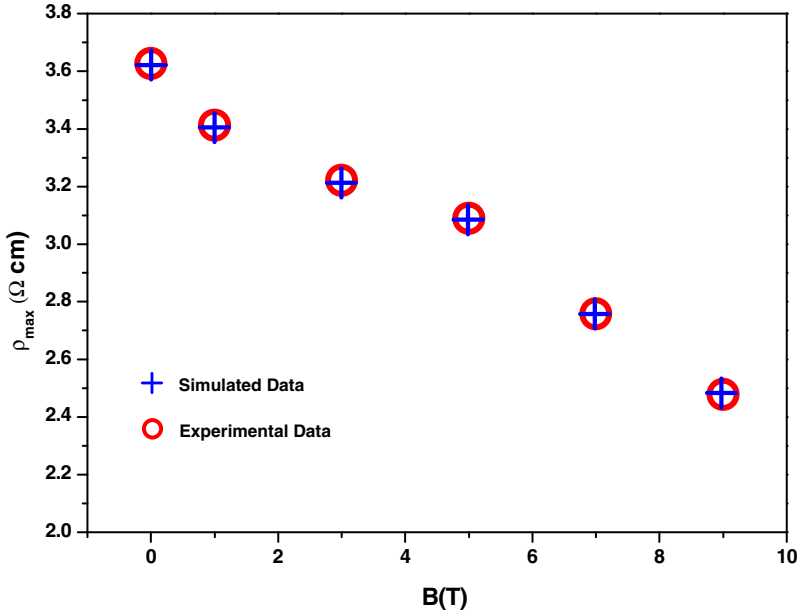

Figure 4 Simulated and measured maximum resistivity as a function of magnetic field.

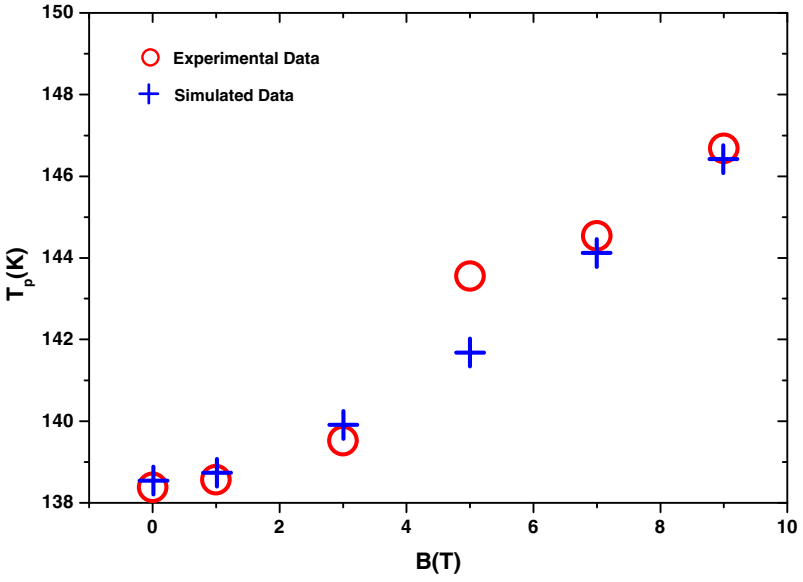

Figure 5 Simulated and measured metal–insulator transition temperatures as a function of magnetic field.

port between manganese and oxygen pairs; so, T_p was shifted to higher temperatures.

It seems that the theoretical results for T_p derived from Eq. (7) were proportional to the experimental results from Table 1. Hence, it can be concluded that magnetic field and metal–insulator transition temperature were correlated. Therefore, using Eq. (7) for investigating the potential shifts of T_p by applying magnetic field seems to be useful. Also, Eq. (7) can be used in order to predict T_p before applying the magnetic field. Designing and building temperature-based sensors using Eq. (7) will be possible as well.

4. Conclusion

In this paper, electrical resistivity of the bi-layered manganite $LaSr_2Mn_2O_7$ in the temperature range around the metal–insulator transition temperature was fitted using Gauss function. Based on the current investigations, it was found that Gauss function not only could describe the behavior of the electrical resistivity as a function of temperature in the measured area, but could also predict some electrical behaviors of $LaSr_2Mn_2O_7$. Using this mathematical model on the experimental data of this specimen along with its proper accommodation may

also make finding the relationships between the magnetic field and metal–insulator transition temperature for other similar manganites possible.

References

Al-Habahbeh, O.M., Mohammad, A., Al-Khalidi, A., Khanfer, M., Obeid, M., 2018. Design optimization of a large-scale thermoelectric generator. J. King Saud Univ. Eng. Sci. 30 (2), 177–182.

Anderson, P.W., Hasegawa, H., 1955. Considerations on double exchange. Phys. Rev. 100, 675.

Ang, R., Zhang, R.L., Zha, B.C., Zhu, X.B., Song, W.H., Sun, Y.P., 2006. Effects of Cr doping in bilayered manganite $LaSr_2Mn_2O_7$: resistivity, thermoelectric power, and thermal conductivity. J. Solid State Commun. 137, 492.

Changshi, L., 2011. Prediction of the magneto-resistance of $La_{0.67}Ca_{0.33}MnO_3$ and $La_{0.8}Sr_{0.2}MnO_3$ via temperature and a magnetic field. J. Chem. Eng. Data 56, 2.

Chen, X.J., Zhang, C.L., Gardner, J.S., Sarrao, J.L., Almasan, C.C., 2002. Small-polaron hopping conduction in bilayer manganite $La_{1.2}Sr_{1.8}Mn_2O_7$. Phys. Rev. B 67, 094426.

Chen, X.J., Zhang, C.L., Gardner, J.S., Sarrao, J.L., Almasan, C.C., 2003. Variable-range hopping conductivity of the half-doped bilayer manganite $LaSr_2Mn_2O_7$. Phys. Rev. B 68, 064405.

Ehsani, M.H., Ghazi, M.E., Kameli, P., 2012a. Effects of pH and sintering temperature on the synthesis and electrical properties of the bilayered $LaSr_2Mn_2O_7$ manganite prepared by the sol–gel process. J. Mater. Sci. 47, 5815.

Ehsani, M.H., Kameli, P., Ghazi, M.E., 2012b. Influence of grain size on the electrical properties of the double-layered $LaSr_2Mn_2O_7$ manganite. J. Phys. Chem. Solids 73 (744).

Ehsani, M.H., Kameli, P., Ghazi, M.E., Razavi, F.S., Taheri, M., 2013a. Tunable magnetic and magnetocaloric properties of $La_{0.6}Sr_{0.4}MnO_3$ nanoparticles. Appl. Phys. 114, 223907.

Ehsani, M.H., Kameli, P., Ghazi, M.E., Singh, M.P., Razavi, F.S., 2013b. A study of structural and physical properties of heavily co-doped $LaSr_2Mn_2O_7$ bi-layered manganite. J. Supernova. Mag. 26, 2771.

Ehsani, M.H., Jalali Mehrabad, M., Kameli, P., Ghazi, M.E., Razavi, F.S., 2016. Low-temperature electrical resistivity of bilayered. J. Low Temp. Phys., 1–12 http://dx.doi.org/10.1007/s10909-016-1520-1.

Feng, J., Che, P., Wang, J.P., Liu, M.F., Cao, X.Q., 2005. Effect of Ti doping on magnetic properties and magnetoresistance in $LaSr_2Mn_2O_7$. J. Alloys Compd. 397, 220.

Goodenough, J.B., 1955. Theory of the role of covalence in the perovskite-type manganites [La, M(II)]MnO_3. Phys. Rev. 100, 564.

Gupta, A.K., Kumar, V., Khare, N., 2007. Hopping conduction in double layered $La_{2-2x}Ca_{1+2x}Mn_2O_7$ manganite. J. Solid State Sci. 9, 817.

Isaac, S.P., Mathur, N.D., Evetts, J.E., Blamire, M.G., 1998. Magnetoresistance of artificial $La_{0.7}Sr_{0.3}MnO_3$ grain boundaries as a function of misorientation angle. Appl. Phys. Lett. 72, 2038.

Liu, S., Guillet, B., Aryan, A., Adamo, C., Routoure, J.-M., Lemarie, F., Schlom, D.G., Mechin, L., 2013. $La_{0.7}Sr_{0.3}MnO_3$ suspended microbridges for uncooled bolometers made using reactive ion etching of the silicon substrate. Microelectron. Eng. 111, 101.

Mitchell, J.F., Argyriou, D.N., Berger, A., Gray, K.E., Osborn, R., Welp, U., 2001. Spin, charge, and lattice states in layered magnetoresistive oxides. J. Phys. Chem. B 105, 10731.

Moritomo, Y., Asamitsu, A., Kuwahara, H., Tokura, Y., 1996. Low temperature electrical transport in double layered CMR manganite $La_{1.2}Sr_{1.4}Ba_{0.4}Mn_2O_7$. Nature 380, 141, London.

Nair, S., Banerjee, A., 2004. Dilution of two-dimensional antiferromagnetism by Mn site substitution in $La_1Sr_2Mn_{2-x}Al_xO_7$. Phys. Rev. B 70, 104428.

Panwar, S., Kumar, V., Chaudhary, A., Kumar, R., Singh, I., 2015. Study of magnetotransport properties of colossal magnetoresistive manganites ($Re_{1-x}A_xMnO_3$): a variational treatment. J Solid State Commun. 223, 32.

Ramirez, A.P., 1997. Colossal magnetoresistance. J. Phys.: Condens. Matter 9, 8171.

Seshadri, R., Maignan, A., Hervieu, M., Nguyen, N., Raveau, B., 1997. Complex magnetotransport in $LaSr_2Mn_2O_7$. Solid State Commun. 101, 453.

Yaremchenko, A.A., Bannikov, D.O., Kovalevsky, A.V., Cherepanov, V.A., Kharton, V.V., 2008. High-temperature transport properties, thermal expansion and cathodic performance of Ni-substituted $LaSr_2Mn_2O_7$. J. Solid State Chem. 181, 3024.

Zener, C., 1951. Interaction between the *d*-shells in the transition metals. II. ferromagnetic compounds of manganese with perovskite structure. Phys. Rev. 82, 403.

Zhang, R.L., Song, W.H., Dai, J.M., Sun, Y.P., 2004a. Structural, magnetic and transport properties of the Cu-doped manganites $La_{0.85}Te_{0.15}Mn_{1-x}Cu_xO_3$. Phys. Rev. B 70, 224418.

Zhang, R.L., Zhao, B.C., Song, W.H., Ma, Y.Q., Yang, J., Sheng, Z. G., Dai, J.M., Sun, Y.P., 2004b. Influence of Co doping on the charge-ordering state of the bilayered manganite $LaSr_2Mn_2O_7$. J. Appl. Phys. 96, 4965.